The antiangiogenic factor 16K hPRL induces endothelial cell cycle arrest by acting at both the G0-G1 and the G2-M phases

Abbreviated title:
16K hPRL induces cell cycle arrest
Authors' name:
Sébastien P. Tabruyn, Ngoc-Quynh-Nhu Nguyen, Anne M. Cornet, Joseph A. Martial‡ and Ingrid Struman.

Laboratoire de Biologie Moléculaire et de Génie Génétique
CBIG (Center of Biomedical Integrative Genoproteomic)
Université de Liège
Allée du 6 Août B6A
B-4000 Liège, Belgium

‡Corresponding author and requests for reprints
Joseph Martial
Laboratoire de Biologie Moléculaire et de Génie Génétique
Université de Liège
Allée du 6 Aout B6A
B-4000 Liège, Belgium
Tel :0032-4-3663371
Fax : 0032-4-3662968
jmartial@ulg.ac.be

Key words : 16K hPRL, anti-angiogenic, cell cycle.

We thank M. Lion for her excellent technical assistance and for 16K hPRL production.
This work was supported by grants from the FRIA ("Fond pour la recherche industrielle et agricole") (to ST, NQNN), Télévie (to ST), FNRS ("Fond national pour la recherche scientifique") (to IS), the Fédération Belge contre le Cancer and the Université de Liège (Fonds Spéciaux).

ABSTRACT

The 16-kDa N-terminal fragment of human prolactin (16K hPRL) is a potent antiangiogenic factor that has been shown to prevent tumor growth in a xenograph mouse model. In this paper we first demonstrate that 16K hPRL inhibits serum-induced DNA synthesis in adult bovine aortic endothelial (ABAE) cells. This inhibition is associated with cell cycle arrest at both the G0-G1 and the G2-M phase. Western blot analysis revealed that 16K hPRL strongly decreases levels of cyclin-D1 and cyclin-B1, but not cyclin-E. The effect on cyclin-D1 is at least partially transcriptional, since treatment with 16K hPRL both reduces the cyclin-D1 mRNA level and down-regulates cyclin-D1 promoter activity. This regulation may be due to inhibition of the MAPK pathway, but it is independent of the GSK-3β pathway. Lastly, 16K hPRL induces the expression of negative cell cycle regulators: the CDK inhibitors p21(cip1) and p27(kip1). In summary, 16K hPRL inhibits serum-induced proliferation of endothelial cells through combined effects on positive and negative regulators of cell cycle progression.

INTRODUCTION

Angiogenesis, the formation of new blood vessels from pre-existing ones, is necessary for many physiological processes, including embryonic vascular development and differentiation, wound healing, and organ regeneration. On the other hand, angiogenesis is also associated with pathological conditions such as cancer, rheumatoid arthritis, diabetic retinopathy, and atherosclerosis (1). Many angiogenic inhibitors are currently in clinical trials of treatments for such pathologies. Recently, some have received FDA approval (2). These inhibitors act by different mechanisms, including inhibition of proliferation, induction of apoptosis, or inhibition of migration. Better understanding of the basic mechanisms of action of inhibitors will lead to developing effective antiangiogenic therapy.

We have shown previously that recombinant 16-kDa N-terminal fragments of human PRL/GH-family members (like those of prolactin (16K PRL), growth hormone (16K GH), variant GH (16K GH-v), and placental lactogen (16K PL)) show antiangiogenic properties (3). New data strongly suggest that 16K hPRL has potential as an anti-cancer drug: in $Rag1^{-/-}$ mice having received a subcutaneous implant of HCT116 human colon cancer cells stably transfected with an expression vector encoding 16K hPRL, expression and secretion of biologically active 16K hPRL led to inhibition of tumor growth and neovascularization (4). Furthermore, using an adenovirus transfer vector, Kim *et al*. have shown that expression of 16K hPRL in prostate cancer cells reduce markedly their ability to form tumors in a xenograft mouse model (5). Recently, 16K hPRL was shown to prevent angiogenesis in a non-cancer angiogenesis-dependent disease: administered by means of adenovirus-mediated gene transfer, it proved able to prevent retinal neovascularization in a mouse model of oxygen-induced retinopathy (6).

To date, the mechanisms underlying the anti-angiogenic action of 16K hPRL are only partially known. In capillary endothelial cells, the antiangiogenic effect appears to be mediated by a saturable high-affinity 16K hPRL binding site - as yet unknown but distinct from the PRL receptor (7). The formation of new microvasculature requires activation of proteases, including urokinase (uPA). Lee *et al*. have shown that 16K hPRL inhibits uPA activation by increasing expression of type 1 plasminogen activator inhibitor (PAI-1) (8).

Among the different biological processes leading to inhibition of angiogenesis, two of the most effective are induction of apoptosis and inhibition of cell proliferation. These may explain the effects of the most powerful inhibitors of angiogenesis. Martini *et al.* have demonstrated that 16K hPRL induces apoptosis of endothelial cells (9). Signaling events associated with 16K hPRL-induced apoptosis include increased DNA fragmentation and activation of caspase-1 and caspase-3. Recently we demonstrated that NF-κB activation plays a key role in the mechanism by which 16K hPRL induces apoptosis in vascular endothelial cells. We showed that NF-κB activation is required for the activation of caspase-8 and caspase-9, which in turn trigger caspase-3 activation and DNA fragmentation (10). Less studied are the mechanisms by which 16K hPRL prevents endothelial cell proliferation. Up to now, only one molecular mechanism has been linked to the anti-proliferative effect of 16K hPRL: inhibition by 16K hPRL of VEGF-induced Ras activation, causing MAPK activation to be blocked (11).

The control of cell proliferation by extracellular signals may occur at checkpoints located at different phases of the cell cycle. It is exerted by cyclin, cyclin-dependent kinases (CDKs), and CDK inhibitors (CKI). Cell cycle progression is triggered by the activation of different CDKs. The association of CDKs with cyclins and inhibitors determines these activations. For example, cyclin-D and cyclin-E, in association with CDK4 and CDK6, contribute to the G1/S transition, whereas inhibition of the kinase activity of cyclin/CDK complex is mediated by several CKIs, including p21(cip1) and p27(kip1) (12).

In this paper we demonstrate that 16K hPRL can induce cell cycle arrest in endothelial cells. By flow cytometry analysis, we show that this arrest occurs at both the G1/S and G2/M transitions. These blockades seem to be caused, respectively, by

down-regulation of cyclin-D1 and cyclin-B1. Down-regulation of cyclin-D1 may result from the inhibition of serum-induced activation of the MAPK pathway. We further identify p27(kip1) and p21(cip1) as key potential mediators in 16K hPRL-induced multi-phase cell cycle arrest.

RESULTS

16K hPRL inhibits DNA synthesis in endothelial Cells

Previous studies have shown that 16K hPRL can inhibit bFGF-stimulated growth of cultured endothelial cells (13). In the present work, we stimulated ABAE cell proliferation with fetal bovine serum (FBS), which contains many growth factors and cytokines that promote signaling through multiple pathways. To examine the effect of 16K hPRL on serum-induced proliferation of ABAE cells, we synchronized ABAE cells by subjecting them to a 48-h contact inhibition period and then allowed cell cycle progression by replating the cells in medium containing 10% FBS.

First, cell proliferation was assessed by measuring ^{3}H-thymidine incorporation into DNA (Fig 1A). FBS at 10% concentration substantially induced ^{3}H-thymidine incorporation. Treatment with increasing concentrations of 16K hPRL for 16 h inhibited this incorporation in a dose-dependent manner. The amount of ^{3}H-thymidine incorporated into cells treated with the highest concentration of 16K hPRL (10 nM) was similar to that observed in cells cultured for 16 h in the absence of serum (0% FBS) (data not shown). As the 16K hPRL used in these experiments was produced in *Escherichia coli*, it was necessary to demonstrate that the observed effects were not due to bacterial endotoxin. The amount of endotoxin (0.02 ng/ml) present in 10 nM 16K hPRL (Endo-C) was found to cause only a slight decrease in ^{3}H-thymidine incorporation that could not account for the observed effect of the 16K hPRL preparation. To further dissociate the action of 16K hPRL from contaminants in the preparation, immunoneutralization experiments were carried out (Fig 1B). The 16K hPRL (10 nM) activity was abolished when 16K hPRL was preincubated with polyclonal antiserum raised against 16K hPRL before the addition to the cell culture. This immunoneutralization is dose-dependent since increasing dilution of the antiserum progressively restores the 16K hPRL activity. This experiment demonstrates that the ability of 16K hPRL to inhibit DNA synthesis is dependent on the peptide activity and not on endotoxin or any other eventual contaminant proteins present in the preparation.

To study more precisely the effect of 16K hPRL on cell proliferation, we used flow cytometry to determine the proliferation state of single cells, and hence to estimate the percentage of proliferating adherent cells (Fig 1C). Stimulation with 10% FBS was found to induce a large increase (from 25% to 49%) in the percentage of cells having incorporated BrdU. Simultaneous incubation with 10 nM 16K hPRL for 16 h strongly decreased this cell population (from 49% to 16%). This effect was unrelated to endotoxin contamination. From these two experiments, we conclude that 16K hPRL can abolish serum-stimulated DNA synthesis.

16K hPRL induces G0-G1 and G2-M arrest in endothelial cells

In both the above experiments and previous studies, 16K hPRL-triggered inhibition of cell proliferation was estimated by measuring, directly or indirectly, the extent to which 16K hPRL treatment reduces cell number. The assays on which this work was based measure cell numbers indirectly on the basis of DNA synthesis. Yet a decrease in cell number can result from inhibition of mitosis, induction of apoptosis, or both. These experiments should be interpreted with caution in the light of recent results showing that 16K hPRL, under some culture conditions, is a potent inducer of endothelial cell apoptosis. To clarify this question, we examined whether 16K hPRL can affect the cell cycle distribution of ABAE cells (Fig 2A). Under our culture conditions, addition of 10% FBS to G0-synchronized ABAE cells allowed their entry into the S phase after an incubation period of approximately 14 h. The S-phase population reached a maximum (31%) after 16 or 18 h (data not shown). Treatment with 10 nM 16K hPRL led to a significant decrease in the proportion of cells in the S phase after this period (11%). The absence of subdiploid cells indicated that 16K hPRL did not significantly induce apoptosis under these conditions. Because the cell cycle might also be arrested at the G2/M transition, we performed another experiment in which synchronized ABAE cells were first treated with 10% FBS for 16 h in order to reach a maximum of cells in the S phase, then exposed to 10 nM 16K hPRL for 8 h (Fig 2B). Under these conditions, the proportion of cells in the G2 phase (36%) was higher than when cells were incubated with FBS only (22%). From these analyses, we conclude that 16K hPRL induces cell cycle arrest at both the G1/S and G2/M transitions.

16K hPRL reduces the level of cyclin-D1 but not that of cyclin-E.

We further investigated the mechanisms involved in this multi-phase cell cycle arrest. The importance of cyclin-D1 and cyclin-E in cells transitioning from G1 into S has been widely demonstrated (14). We first measured levels of the cyclin-E (Fig 3A) and cyclin-D1 proteins (Fig 3B) in cells incubated or not with 16K hPRL for various lengths of time (from 6 to 24 h). In untreated cells, cyclin-D1 and cyclin-E levels were maximal after 12 h of incubation with 10% FBS. This time course is in agreement with the role of cyclin-D1 and cyclin-E in the G1-to-S-phase transition. Treatment with 16K hPRL did not modify the time course of the cyclin-E level. In contrast, it did result in lower levels of cyclin-D1. This reduction was observed already after 6 h and remained considerable up to hour 24. To further analyze the effect of 16K hPRL on cyclin-D1, we treated ABAE cells for 16 h with increasing 16K hPRL concentrations (from 2 to 10 nM). 16K hPRL was found to decrease the cyclin-D1 level in a dose-dependent manner (Fig 3C). Endotoxin tested at 0.02 ng/ml (the concentration present in the highest dose of 16K hPRL) had no significant effect (Fig 3D).

16K hPRL affects the level of cyclin-D1 mRNA and inhibits cyclin-D1 promoter activity.

Previous data have demonstrated both protein-level and mRNA-level regulation of cyclin-D1. By Northern blot analysis we determined the cyclin-D1 mRNA level in ABAE cells exposed or not to 16K hPRL (Fig 4A). Treatment for 8 h with 10 nM 16K hPRL was found to decrease the cyclin-D1 mRNA level. As such an effect might reflect reduced transcription, reduced stability, or both, we transfected ABAE cells with a cyclin-D1 promoter reporter construct (CD1-Luc) and examined the effect of 16K hPRL on activation of this promoter (Fig 4B). Treatment with 16K hPRL was found to down-regulate transcriptional activation in a dose-dependent manner. The highest 16K hPRL concentration (10 nM) reduced activation of the cyclin-D1 promoter by 50%. The amount of endotoxin present in the highest dose of 16K hPRL caused no significant reduction in cyclin-D1 promoter activation. Taken together, these results show that 16K hPRL decreases both the level of cyclin-D1 and that of cyclin-D mRNA, probably by interfering with transcriptional activation of the cyclin-D1 promoter.

Involvement of the MAPK pathway in 16K hPRL-triggered cell cycle arrest

Among the pathways that might regulate transcription of the gene coding for cyclin-D1, the GSK-3β and MAPK pathways are the most important. We therefore tested the ability of 16K hPRL to interfere with one or both of these pathways and thus to inhibit transcription of the cyclin-D1 gene.

GSK-3β might down-regulate the cyclin-D1 at both the protein level, by inducing its degradation, and the mRNA level, by inducing β-catenin degradation. GSK-3β kinase activity is regulated by its phosphorylation state. Unlike most kinases, GSK-3β is active in resting cells; stimulation with mitogens or growth factors leads to its inactivation by phosphorylation of the serine residue at position 9 (15). To investigate whether 16K hPRL can inhibit this phosphorylation and activate GSK-3β, we

performed Western blot analysis with an antibody raised against Ser9-phosphorylated GSK-3β (Fig 5A). In this experiment, treatment for various times (from 0 to 6 h) with 10 nM 16K hPRL failed to abolish phosphorylation of GSK-3β on serine 9. The total GSK-3β level also remained unaltered by 16K hPRL treatment.

Since β-catenin is degraded following phosphorylation by GSK-3β (16), we measured the level of β-catenin in nuclear extracts of ABAE cells treated for various times with 10 nM 16K hPRL (from 0 to 6 h) (Fig 5B). Treatment with 16K hPRL caused no significant modification of the β-catenin level. This confirms that the effect of 16K hPRL on the cyclin-D1 level is not due to interference with the GSK-3β pathway.

Previous studies suggest that cyclin-D1 can also be regulated by the MAPK pathway, ERK1 and ERK2 activations having been shown to increase transcription of the cyclin-D1 gene (17). To determine the effect of serum on MAPK pathway activation, we exposed serum-deprived ABAE cells to 10% FBS for 0 to 3 h (Fig 5C). Western blot analysis with an antibody raised against the phosphorylated forms of ERK1 and ERK2 revealed the following pattern: ERK1/2 activation within 20 minutes, a decrease to near basal phosphorylated ERK over the next hour, these levels being maintained for the next 2 h. Controls showed that levels of total ERK1 and ERK2 remained unaltered. This result indicates that serum can activate ERK1/2 but that activation is restricted in time. We then tested whether 16K hPRL can inhibit serum-induced activation of ERK1 and ERK2, as shown for stimulation with bFGF (18). Treatment with 10 nM 16K hPRL was found to inhibit serum-induced as well as bFGF-induced ERK activation (Fig 5D). No treatment had any effect on the total level of ERK-1 or ERK-2. This experiment highlights a potential role of the MAPK pathway in 16K hPRL regulation of the cyclin-D1 level.

16K hPRL down-regulates cyclin-B1.

Cyclin-B1 is required for the activation of mitosis. To examine whether the G2-M cell cycle arrest induced by 16K hPRL might be triggered by an altered level of cyclin-B1, we analyzed by Western blotting cells treated or not with 10 nM 16K hPRL (Fig 6A). In untreated cells, the cyclin-B1 level began to rise at 12 h and peaked at 24 h. This time course is in agreement with previous studies on eukaryotic cells, indicating that the level of cyclin-B1 protein is minimal in G1, rises in S, and peaks in the G2 phase (19). Cells treated with 16K hPRL showed a strongly reduced cyclin-B1 level at all times (Fig 6B). This effect was unrelated to endotoxin contamination (Fig 6C). Down-regulation of cyclin-B1 may be explained by the observed G0-G1 cell cycle arrest caused by 16K hPRL treatment. To clarify this question, we used flow cytometry to determine the level of cyclin-B1 in G2-phase cells (Fig 6C). ABAE cells were first incubated with 10% FBS for 16 h in order to reach a maximum of cells in the S phase, then treated with 10 nM 16K hPRL for 8 h. Cells blocked in the G2 phase in response to 16K hPRL treatment displayed a lower cyclin-B1 level than untreated G2-phase cells. This last experiment supports the view that 16K hPRL induces a G2 cell cycle arrest by down-regulating cyclin-B1.

16K hPRL up-regulates p27(kip1) and p21(cip1)

Cell cycle inhibitors, including Cip/Kip proteins such as p21(cip1) and p27(kip1), exert a negative control on various cyclin-CDK complexes. The two inhibitors just mentioned have been shown to inhibit both the G1/S and G2/M transitions (20). As p27(kip1) is controlled mainly at a post-transcriptional level (21), we examined its level by Western blotting in ABAE cells treated or not with 16K hPRL (Fig 7A). In untreated cells, the p27(kip1) level was high at 6 h, lower at 12 h, and remained low to hour 24. In the presence of 16K hPRL, the p27(kip1) level remained high over this entire period. To characterize this process, we treated ABAE cells for 16 h with increasing concentrations of 16K hPRL (Fig 7B). Western blot analysis showed higher p27(kip1) levels in 16K hPRL-treated cells. The effect was dose-dependent and unrelated to endotoxin contamination (Fig. 7C). We conclude that 16K hPRL treatment causes the p27(kip1) level to rise in ABAE cells.

To investigate whether 16K hPRL induces up-regulation of p21(cip1), ABAE cells were treated for various lengths of time (from 0 to 6 hours) with 10 nM 16K hPRL and Northern blot analysis was performed (Fig 8A). We observed an increased p21(cip1) mRNA level at 2 h, maintained at 4 h and beginning to decline at 6 h. To further characterize the effect of 16K hPRL on p21(cip1), we stimulated ABAE cells for 2 h with increasing concentrations of 16K hPRL (from 2 to 10 nM) (Fig 8B). 16K hPRL was found to increase the p21(cip1) mRNA level in a concentration-dependent manner. The effect was unrelated to the presence of endotoxin (Fig 8C).

DISCUSSION

We have observed an inhibition of DNA synthesis in 16K hPRL-treated endothelial cells. To better understand the signaling mechanisms involved, we have focused here on how 16K hPRL affects cell cycle progression and on molecules that regulate this process.

We show that 16K hPRL acts at more than one phase of the cell cycle. Our flow cytometry analysis of endothelial cells labeled with propidium iodide shows that 16K hPRL blocks the cell cycle at both the G0/G1 and G2/M transitions. This dual effect highlights the potent antiproliferative effect of 16K hPRL and suggests that 16K hPRL might stop proliferation of an endothelial cell whatever its stage in the cell cycle. To our knowledge, curcumin is the only other antiangiogenic molecule shown to trigger G0-G1- and G2-M-phase cell cycle arrest in endothelial cells (ECV-304 cells) (22).

In the present study, proliferation was induced by a large concentration of fetal bovine serum. Although serum contains many growth factors and cytokines that can induce proliferation through multiple pathways, 16K hPRL is able to abolish serum-induced progression of endothelial cells through the cell cycle. On this basis we hypothesize that 16K hPRL acts powerfully on the cell cycle via different pathways.

Cell cycle progression is controlled by several CDK complexes, such as cyclin-D1/CDK4 and cyclin-E/CDK2 in the G1/S transition and cyclin-B1/CDK1 in the G2/M transition. The activities of these complexes depend on the balance between cyclins and CKIs such as p27(kip1) and p21(cip1) (20). To examine whether 16K hPRL-triggered inhibition of cell proliferation is caused by cyclin down-regulation, CKI up-regulation or both, we have analyzed the expression of these cell cycle regulators in ABAE cells treated with 16K hPRL. Our studies reveal that treatment with 16K hPRL results in a significant down-regulation of cyclin-D1 and cyclin-B1, but we have not found any evidence of an effect on cyclin-E.

Down-regulation of cyclin-D1 occurs at least at the transcriptional level, since 16K hPRL treatment reduces the cyclin-D1 mRNA level and cyclin-D1 promoter activity. Many studies have shown that the transcriptional regulation of cyclin-D1 can be attributed to various pathways, notably the MAPK (23) and GSK-3β (24) pathways. GSK-3β is a multifunctional protein kinase that can alter the cyclin-D1 level by several mechanisms. Active GSK-3β phosphorylates cyclin-D1 at Thr286 to promote its export from the nucleus and subsequent proteasomal degradation. GSK-3β can also degrade β-catenin, preventing it from activating transcription of cyclin-D1 by association with the TCF transcription factor (25). The GSK-3β pathway does not appear to be altered by 16K hPRL, since levels of phospho-GSK-3β and nuclear β-catenin remain unchanged after treatment with 16K hPRL. The MAPK pathway, on the other hand, is affected by 16K hPRL treatment: our analysis of the phosphorylation state of ERK1 and ERK2 in the presence and absence of 16K hPRL suggests that 16K hPRL can inhibit serum-induced activation of this pathway. Since activated ERK1/2 trigger a cyclin-D1 level increase by translocating to the nucleus and phosphorylating transcription factors like the Ets and AP-1 family members (26), we suggest that 16K hPRL down-regulates cyclin-D1 by interfering with the MAPK pathway.

We have further examined the ability of 16K hPRL to cause cell cycle arrest at the G2/M transition by analyzing cyclin-B1 production. Cyclin-B1 is a key regulator of the cell cycle, central to controlling the G2/M transition. Cyclin-B1 is involved in regulating the events of mitosis. Its synthesis, which is increased in the early G2 phase, is necessary for transition from G2 through M (27). Here we show that ABAE cells arrested in G2-M have a reduced cyclin-B1 content. Our results suggest that this reduction leads to accumulation of endothelial cells in the G2 phase and inhibits transition to the M phase.

Our data also demonstrate a significantly increased level of p27(kip1) protein and p21(cip1) mRNA in 16K hPRL-treated endothelial cells. It has been reported previously that these two inhibitors may inhibit both the G1/S and G2/M transitions (20). For lack of a good antibody against bovine p21(cip1) we were unable to detect this protein in our bovine endothelial cells. Nevertheless, since the main regulation of p21(cip1) appears to be transcriptional (28), we believe that the increased p21(cip1) mRNA level observed in response to 16K hPRL is likely to correlate with an increased level of p21(cip1) protein.

The precise mechanism by which 16K hPRL induces p21(cip1) and p27(kip1) remains to be determined. Despite many studies demonstrating that regulation of p21(cip1) involves p53, other studies show that NF-κB may also be involved in this process. NF-κB is a transcription factor involved in the response of cells to various stimuli. It plays a central role in the immune and inflammatory responses, apoptosis, and proliferation (29). The human p21(cip1) promoter contains a functional NF-κB site (30). In addition, NF-κB activation can cause cell cycle arrest of primary keratinocytes through induction of p21(cip1) (31). As we have previously shown that 16K hPRL can activate NF-κB in endothelial cells (10), one might expect NF-κB to play a role in the induction of p21(cip1) in response to 16K hPRL.

We have also shown previously that full-length PRL and 16K PRL exert opposite effects on endothelial cells as regards angiogenesis (3). Several studies have probed the effect of full-length PRL on proliferation. As PRL stimulates cell cycle progression in epithelial tumor cells by up-regulating cyclin-D1 and cyclin-B1 and down-regulating p21(cip1) (32), it might be interesting to determine whether this also occurs in endothelial cells.

In conclusion, this is the first study showing that 16K hPRL inhibits the cell cycle at more than one phase through combined effects on positive (cyclin-D1, cyclin-B1) and negative (p21(cip1) and p27(kip1)) regulators of CDK. This dual mechanism of action suggests that 16K hPRL might have potential as a potent anticancer drug. Tumor-triggered angiogenesis may indeed be driven by many different angiogenic factors subject to regulation by different environmental and/or genetic factors. Hence, different tumors are likely to respond differently to an antiangiogenic drug. With 16K hPRL we have an antiangiogenic compound that blocks serum-induced proliferation at more than one cell-cycle checkpoint and via more than one pathway. Used as an antiangiogenic anticancer agent, it might thus show a fairly broad action spectrum.

.

MATERIALS AND METHODS

Production of recombinant protein and antibody

Recombinant 16K hPRL was produced and purified from *E. coli* as previously described (10). The purity of the recombinant protein exceeded 95% (as estimated by Coomassie Blue staining) and the endotoxin level was 0.125 pg/ng recombinant protein, as quantified with "the rapid endo test" of the European endotoxin testing service (Cambrex Bioproducts Europe). *E. coli* (serotype 055:B5) endotoxin was purchased from Sigma. In experiments where the action of 16K hPRL was compared with that of endotoxin, the amount of endotoxin used was the amount present in the highest 16K hPRL concentration used in the assay. The anti-16K hPRL antiserum used (no. 602) is a rabbit polyclonal antibody recognizing 16K hPRL.

Cell cultures

ABAE (adult bovine aortic endothelial) cells were isolated as previously described (37). The cells were grown and serially passaged in low-glucose Dulbbecco's modified Eagle's medium containing 10% fetal bovine serum (FBS) and 100 U/ml penicillin/streptomycin (10% FCS medium). Recombinant human basic FGF (bFGF, Sigma) was added (1 ng/ml) to the culture every other day. Confluent cells corresponding to passages 8 to 13 were used in the experiments.

Measurement of [3H]-thymidine incorporation.

ABAE cells were growth-arrested by contact inhibition for 48 h. The cells were harvested, plated in 24-well plates (3×10^4/well), and treated with 16K hPRL or endotoxin at the indicated doses. In the last 3 h of treatment, 1 µCi/ml [methyl-^{3}H]thymidine was added (specific radioactivity 6.7 Ci/mmol; ICN). Thereafter, the cells were washed with ice-cold 5% trichloroacetic acid and incubated on ice for 20 min in 5% trichloroacetic acid. After two washes with ice-cold 5% trichloroacetic acid, the cells were solubilized with 0.25 N NaOH and transferred to counting vials containing 3 ml scintillation fluid (Ecolite, ICN).

BrdU incorporation analysis.

ABAE cells were growth-arrested by contact inhibition for 48 h. The cells were harvested and plated in a 100-mm plate (5×10^5/plate) for 18 h in medium containing 0 or 10% FBS with or without 16K hPRL or endotoxin. 10 µM BrdU was added to the cells during the last 3 h. BrdU incorporation was measured by means of the Fluos In Situ Cell Proliferation Kit (Roche Applied sciences) according to the manufacturer's instructions. Briefly, the cells were washed with PBS and harvested by trypsinization. They were then washed again with PBS, fixed with cold 70% ethanol for 1 h, and centrifuged. The pellet was resuspended in 2 N HCl and incubated at room temperature for 30 min. The cells were washed with PBS and incubated at room temperature for 45 min with a fluorescein-conjugated monoclonal anti-BrdU antibody. They were then washed with PBS, centrifuged, and resuspended in PBS before analysis with a Coulter Epics XL flow cytometer equipped with an argon laser emitting at 488 nm. Green fluorescence intensity (FL1) was measured using a 530 nm + 15 nm band pass filter. Graphical and population analyses were performed with FlowJo version 6.01 software (TreeStar).

Cell cycle analysis

ABAE cells were growth-arrested by contact inhibition for 48 h. The cells were harvested, plated (5×10^5/plate) in a 100-mm plate, and incubated for 16 h in medium containing 0 or 10% FCS, with or without 16K hPRL or endotoxin. They were then harvested and fixed in ice-cold ethanol for 2 h at 4°C before being centrifuged and incubated (at 37 °C for 30 min) in PBS containing Rnase (5 µg/ml) and propidium iodide (50 µg/ml). The cells were analyzed with a Coulter Epics XL flow cytometer equipped with an argon laser emitting at 488 nm. Red fluorescence intensity (FL3) was measured using a 620 + 15 nm band pass filter. Graphical and cell cycle analyses were performed with FlowJo version 6.01 software (TreeStar).

Preparation of cell extracts

For total cell extracts, the cells were harvested, centrifuged, and lysed on ice for 30 min in lysis buffer (25 mM HEPES, pH 7.9, 150 mM NaCl, Triton 0.5%, 1 mM DTT, 1mM PMSF). Insoluble cell debris were removed by centrifugation at 10000 g for 15 min. Nuclear extracts were obtained as previously described (10). Aliquots of protein-containing supernatant were stored at –80°C. Protein concentrations were determined by the Bradford method using the Bio-Rad protein assay reagent.

Western blot analysis

Thirty micrograms of cytoplasmic cell lysate were resolved by SDS/PAGE (12%) and the bands transferred to a Polyvinilidene fluoride membrane (Millipore). The blots were blocked for 1 h with 8% milk in TBS with 0.1% Tween 20 (TBST) and probed for 1 h with primary antibodies: anti-cyclin-D1 (M-20), anti-cyclin E (M-20), anti-cyclin-B1 (GNS1), anti-p27kip1 (C-19), anti-p-GSK-3β (Ser 9), or anti-GSK-3β (0011-A) from Santa-

Cruz Biotechnology, anti p-Erk1/2 (E10) from Cell Signaling Technology, anti-ERK1/2 (CT) from Upstate, or anti-β-catenin from BD Biosciences. After three washes with TBST, antigen-antibody complexes were detected by means of peroxidase-conjugated secondary antibody and an enhanced fluoro-chemiluminescent system (ECL-plus; Amersham Biosciences).

Luciferase reporter assays

ABAE cells were harvested and plated into 24-well plates (3 X 10^4/well). After 24 h, ABAE cells were transfected with 0.4 µg pCD1-Luc reporter plasmid in combination with 0.05 µg pCMV-βgal plasmid. Transfections were performed with Fugene 6 reagent (Roche Applied Sciences) according to the manufacturer's instructions. The pCD1-Luc plasmid contains, upstream from the luciferase gene, the human cyclin D1 promoter as previously described (33). Plasmid pCD1-Luc was kindly provided by R.G. Pestell (Lombardi Comprehensive Cancer Center, Washington, DC). Cells were transfected as described above and treated or not for 16 h with various concentrations of 16K hPRL or endotoxin. ABAE cells were washed once with cold PBS before incubation in 200 µl lysis buffer (25 mM Tris-Phosphate; 8 mM $MgCl_2$; 1 mM EDTA; 1% Triton; 15% Glycerol; 1 mM DTT; 0.2 mM PMSF) for 20 min. Luciferase activity was measured in 100 µl supernatant incubated in the presence of luciferin (Promega), with a 96-well plate reader (Wallac Victor2, PerkinElmer). Luciferase activity was normalized relative to β-galactosidase activity, measured according to the manufacturer's instructions (β-Gal Reporter Gene Assay, Roche Applied Sciences).

Northern blot analysis

Total RNA was extracted using the Rneasy kit (Qiagen) according to the manufacturer's instructions. RNA (10 µg) was resolved on a 1.2% agarose gel containing 10% formaldehyde and transferred to a nylon membrane (HybondTM-N, Amersham Biosciences). The membrane was prehybridized in the solution (50% formamide, 5x SSPE, 10x Denhardt's solution, 2% SDS, 0.1 mg/ml salmon sperm DNA) for 4 h at 42 °C and then hybridized for 18 h with a radiolabeled DNA probe appropriate for detection of cyclin-D1 or p21(cip1) mRNA. The full-length human Cyclin-D1 cDNA used to generate the corresponding probe was kindly provided by A. Miyajima (Institute of Molecular and Cellular Biosciences, University of Tokyo). The full-length human p21(cip1) cDNA was kindly provided by S. Carlson (Lerner Research Institute, Cleveland Clinic Foundation). The probes were labeled with [α-^{32}P] dATP using the Random primers DNA labeling kit (Invitrogen). The membrane was washed twice for 20 min at 25 °C in 2x SSC, 0.05% SDS, twice at 55° in 0.1 X SSC, 0.1% SDS, before visualization with a Molecular Imager Fx (Bio-Rad).

FIGURES

Figure 1: 16K hPRL DNA synthesis of ABAE cells.

Synchronized ABAE cells were plated in 10% FBS medium and treated for 18 h with 16K hPRL. Endotoxin-C (0.02 ng/ml) was added as a control for endotoxin contamination. For the last three hours, cells were incubated with either [^{3}H]thymidine (A,B) or BrdU (C).

A) Dose-response curve for the action of 16K hPRL on [^{3}H]thymidine uptake by ABAE cells. B) 16K hPRL (10 nM) was preincubated with a polyclonal antiserum raised against 16K hPRL at the indicated dilution. The results are expressed as the percentage of 16K hPRL activity. Triplicate samples were analyzed and the data presented are representative of at least three similar experiments. Values are means ±SD. C) Ability of 16K hPRL to prevent DNA synthesis. Detection of BrdU-positive cells by flow cytometry, using the "In Situ Cell Proliferation Kit Fluo" (Roche Applied Sciences) was used to monitor the ability of cells to synthesize DNA. The percentage of BrdU positive cells is defined as the ratio of the number of BrdU-positive cells to the total number, multiplied by 100. The results are representative of three similar and independent experiments.

Figure 2: 16K hPRL induces cell-cycle arrest at both G0-G1 and G2-M.

A) Ability of 16K hPRL to block cells in the G0-G1 phase. Synchronized ABAE cells were plated in medium containing 10% FBS and treated for 16 h with 10 nM 16K hPRL or Endo-C. B) Ability of 16K hPRL to block cells in the G2-M phase. Synchronized ABAE cells were incubated in medium containing 10% FBS for 16 h before addition of 10nM 16K hPRL or Endo-C for 8h. Endo-C (0.02 ng/ml) was added as a control for endotoxin contamination. Cell cycle progression was monitored by detection of DNA content by flow cytometry analysis. ABAE cells were harvested, fixed, and permeabilized. DNA was labeled with propidium iodide. The results are representative of three similar and independent experiments.

Figure 3: 16K hPRL treatment reduces the cyclin-D1 level but not the cyclin-E level.

Levels of the cyclin-D1 and cyclin–E proteins were assessed by Western blot analysis, performed on total protein extracts. All experiments were performed on synchronized ABAE cells plated in medium containing 10% FBS. A) and B): Time courses of cyclin-E (A) and cyclin-D1 (B) protein level variations in ABAE cells treated or not with 16K hPRL (10 nM). C) Dose-response analysis of the effect of 16K hPRL on cyclin-D1 expression after a 16-h treatment. D) Endo-C (0.02 ng/ml) was added as a control for endotoxin contamination, ABAE cells were treated with 16K hPRL (10 nM) or Endo-C for 16 h. All results are representative of three similar and independent experiments.

Figure 4: 16K hPRL affects the level of cyclin-D1 mRNA and inhibits cyclin-D1 promoter activity.

A) Ability of 16K hPRL to reduce the cyclin-D1 mRNA level estimated by Northern blot analysis. Synchronized ABAE cells were plated with 10% FBS and treated for 16 h with 10 nM 16K hPRL. Total RNA was harvested and Northern blot analysis was performed with a human cyclin-D1 cDNA probe. 28S and 18S ribosomal RNA stained with ethidium bromide was used as internal control for the amount of total RNA loaded.

B) Transcriptional regulation cyclin-D1 promoter activity by 16K hPRL. Luciferase activity was measured in ABAE cells transfected with the pCD1-Luc reporter gene vector after incubation for 18 h with increasing concentrations of 16K hPRL. Endo-C (0.02 ng/ml) was added as a control for endotoxin contamination. All luciferase activities are normalized with respect to galactosidase activity. Values for untreated cells are arbitrarily set at 100%. Each bar represents the mean ± SD, n = 3. The results were similar in three independent experiments.

Figure 5: Involvement of the MAPK and GSK-3β pathways in 16K hPRL-induced cell cycle arrest.

Levels of phosphorylated GSK-3β and nuclear β-catenin are not altered in ABAE cells treated with 16K hPRL. Experiments were performed on ABAE cells plated in medium containing 10% FBS. The level of phospho-GSK-3β was estimated by Western blot analysis, performed on total protein extracts. A) Time course of phospho-GSK-3β variation in ABAE cells treated or not with 16K hPRL (10 nM). Normalization was done with an antibody raised against GSK-3β. The level of β-catenin was estimated by Western blot analysis performed on nuclear extracts. B) Time course of β-catenin level variations in ABAE cells treated or not with 16K hPRL (10 nM).

Ability of 16K hPRL to reduce ERK1 and ERK2 phosphorylation estimated by Western blot analysis. ABAE cells were serum starved for 24 h in 0% FBS. D) ABAE cells were stimulated with 10% FBS for various times (0 to 3 h). E) ABAE cells were stimulated for 20 min with 10% FBS or 1 ng/ml bFGF in combination or not with 10nM 16K hPRL. Total protein was harvested and phospho-ERK-1 and phospho-ERK-2 were analyzed by Western blotting. Normalization was done with an ERK-1 and ERK-2 antibody. The results were representative of three similar and independent experiments.

Figure 6: 16K hPRL treatment reduces the cyclin-B protein level.

The level of cyclin-B was estimated in total cell protein extracts by Western blot analysis. Experiments A) and B) were performed on synchronized ABAE cells plated in medium containing 10% FBS. A) Time course of cyclin-B1 level variations. ABAE cells were treated or not for the indicated time

with 10 nM 16K hPRL. B) Endo-C (0.02 ng/ml) was added as a control for endotoxin contamination, ABAE cells were treated with 16K hPRL (10 nM) or Endo-C for 16 h. C) Level of cyclin-B1 in G2-phase cells. Cells were analyzed by flow cytometry for both expression of cyclin-B1 and cell cycle distribution (using a propidium-iodide-labeled DNA content method). Synchronized ABAE cells were incubated for 16 h in medium containing 10% FBS before addition of 10 nM 16K hPRL for 8h. Cells were harvested, permeabilized, fixed, and subjected to immunofluorescence staining with anti-cyclin-B1 antibody prior to analysis by flow cytometry. Only cells in the G2-M phase (as shown for the 16K hPRL treated cells) were analyzed for cyclin-B1 expression. The results are representative of three similar and independent experiments.

Fig 7: 16K hPRL treatment increases the level of p27(kip1) protein
Levels of p27(kip1) protein were estimated by Western blot analysis, performed on total protein extracts. All experiments were performed on synchronized ABAE cells plated in medium containing 10% FBS. A) Time course of p27(kip1)-level variations in ABAE cells treated or not with 16K hPRL (10 nM). B) Dose-response analysis of the effect of 16K hPRL on the p27(kip1) level after a 16-h treatment. C) Endo-C (0.02 ng/ml) was added as a control for endotoxin contamination, ABAE cells were treated with 16K hPRL (10 nM) or Endo-C for 16 h. All results are representative of three similar and independent experiments.

Fig 8: 16K hPRL treatment increases the level of p21(cip1) mRNA
Levels of p21(cip1) mRNA were estimated by Northern blot analysis performed on total cell RNA with a human p21(cip1) DNA probe. Levels of ethidium-bromide-stained rRNA demonstrate similar loading and RNA quality in each lane. A) Time course of p21(cip1) mRNA level variation in ABAE cells treated with 10 nM 16K hPRL B) Dose-response analysis of the effect of 16K hPRL on the p21(cip1) mRNA level after a 2-h treatment. C) Endo-C (0.02 ng/ml) was added as a control for endotoxin contamination; ABAE cells were treated with 16K hPRL (10 nM) or Endo-C for 2 h. All results are representative of three similar and independent experiments.

Bibliography

1. **Carmeliet P** 2003 Angiogenesis in health and disease. Nat Med 9:653-60
2. **Folkman J** 2004 Endogenous angiogenesis inhibitors. Apmis 112:496-507
3. **Struman I, Bentzien F, Lee H, Mainfroid V, D'Angelo G, Goffin V, Weiner RI, Martial JA** 1999 Opposing actions of intact and N-terminal fragments of the human prolactin/growth hormone family members on angiogenesis: an efficient mechanism for the regulation of angiogenesis. Proc Natl Acad Sci U S A 96:1246-51
4. **Bentzien F, Struman I, Martini JF, Martial JA, Weiner RI** 2001 Expression of the antiangiogenic factor 16K hPRL in human HCT116 colon cancer cells inhibits tumor growth in Rag1(-/-) mice. Cancer Res 61:7356-62
5. **Kim J, Luo W, Chen DT, Earley K, Tunstead J, Yu-Lee LY, Lin SH** 2003 Antitumor activity of the 16-kDa prolactin fragment in prostate cancer. Cancer Res 63:386-93
6. **Pan H, Nguyen NQ, Yoshida H, Bentzien F, Shaw LC, Rentier-Delrue F, Martial JA, Weiner R, Struman I, Grant MB** 2004 Molecular targeting of antiangiogenic factor 16K hPRL inhibits oxygen-induced retinopathy in mice. Invest Ophthalmol Vis Sci 45:2413-9
7. **Clapp C, Weiner RI** 1992 A specific, high affinity, saturable binding site for the 16-kilodalton fragment of prolactin on capillary endothelial cells. Endocrinology 130:1380-6
8. **Lee H, Struman I, Clapp C, Martial JA, Weiner RI** 1998 Inhibition of urokinase activity by the antiangiogenic factor 16K prolactin: activation of plasminogen activator inhibitor 1 expression. Endocrinology 139:3696-703
9. **Martini JF, Piot C, Humeau LM, Struman I, Martial JA, Weiner RI** 2000 The antiangiogenic factor 16K PRL induces programmed cell death in endothelial cells by caspase activation. Mol Endocrinol 14:1536-49.
10. **Tabruyn SP, Sorlet CM, Rentier-Delrue F, Bours V, Weiner RI, Martial JA, Struman I** 2003 The antiangiogenic factor 16K human prolactin induces caspase-dependent apoptosis by a mechanism that requires activation of nuclear factor-kappaB. Mol Endocrinol 17:1815-23
11. **D'Angelo G, Martini JF, Iiri T, Fantl WJ, Martial JA, Weiner RI** 1999 16K human prolactin inhibits vascular endothelial growth factor-induced activation of Ras in capillary endothelial cells. Mol Endocrinol 13:692-704
12. **Cheng T** 2004 Cell cycle inhibitors in normal and tumor stem cells. Oncogene 23:7256-66
13. **Ferrara N, Clapp C, Weiner R** 1991 The 16K fragment of prolactin specifically inhibits basal or fibroblast growth factor stimulated growth of capillary endothelial cells. Endocrinology 129:896-900
14. **Stacey DW** 2003 Cyclin D1 serves as a cell cycle regulatory switch in actively proliferating cells. Curr Opin Cell Biol 15:158-63
15. **Cross DA, Alessi DR, Cohen P, Andjelkovich M, Hemmings BA** 1995 Inhibition of glycogen synthase kinase-3 by insulin mediated by protein kinase B. Nature 378:785-9
16. **Manoukian AS, Woodgett JR** 2002 Role of glycogen synthase kinase-3 in cancer: regulation by Wnts and other signaling pathways. Adv Cancer Res 84:203-29
17. **Cheng M, Sexl V, Sherr CJ, Roussel MF** 1998 Assembly of cyclin D-dependent kinase and titration of p27Kip1 regulated by mitogen-activated protein kinase kinase (MEK1). Proc Natl Acad Sci U S A 95:1091-6
18. **D'Angelo G, Struman I, Martial JA, Weiner RI** 1995 Activation of mitogen-activated protein kinases by vascular endothelial growth factor and basic fibroblast growth factor in capillary endothelial cells is inhibited by the antiangiogenic factor 16-kDa N-terminal fragment of prolactin. Proc Natl Acad Sci U S A 92:6374-8
19. **Hwang A, Maity A, McKenna WG, Muschel RJ** 1995 Cell cycle-dependent regulation of the cyclin B1 promoter. J Biol Chem 270:28419-24
20. **Coqueret O** 2003 New roles for p21 and p27 cell-cycle inhibitors: a function for each cell compartment? Trends Cell Biol 13:65-70
21. **Hengst L, Reed SI** 1996 Translational control of p27Kip1 accumulation during the cell cycle. Science 271:1861-4
22. **Park MJ, Kim EH, Park IC, Lee HC, Woo SH, Lee JY, Hong YJ, Rhee CH, Choi SH, Shim BS, Lee SH, Hong SI** 2002 Curcumin inhibits cell cycle progression of immortalized human umbilical vein endothelial (ECV304) cells by up-regulating cyclin-dependent kinase inhibitor, p21WAF1/CIP1, p27KIP1 and p53. Int J Oncol 21:379-83
23. **Ussar S, Voss T** 2004 MEK1 and MEK2, different regulators of the G1/S transition. J Biol Chem 279:43861-9
24. **Ryves WJ, Harwood AJ** 2003 The interaction of glycogen synthase kinase-3 (GSK-3) with the cell cycle. Prog Cell Cycle Res 5:489-95

25. **Novak A, Dedhar S** 1999 Signaling through beta-catenin and Lef/Tcf. Cell Mol Life Sci 56:523-37
26. **Murphy LO, Smith S, Chen RH, Fingar DC, Blenis J** 2002 Molecular interpretation of ERK signal duration by immediate early gene products. Nat Cell Biol 4:556-64
27. **Takizawa CG, Morgan DO** 2000 Control of mitosis by changes in the subcellular location of cyclin-B1-Cdk1 and Cdc25C. Curr Opin Cell Biol 12:658-65
28. **Gartel AL, Goufman E, Tevosian SG, Shih H, Yee AS, Tyner AL** 1998 Activation and repression of p21(WAF1/CIP1) transcription by RB binding proteins. Oncogene 17:3463-9
29. **Shishodia S, Aggarwal BB** 2004 Nuclear factor-kappaB: a friend or a foe in cancer? Biochem Pharmacol 68:1071-80
30. **Hellin AC, Bentires-Alj M, Verlaet M, Benoit V, Gielen J, Bours V, Merville MP** 2000 Roles of nuclear factor-kappaB, p53, and p21/WAF1 in daunomycin-induced cell cycle arrest and apoptosis. J Pharmacol Exp Ther 295:870-8.
31. **Basile JR, Eichten A, Zacny V, Munger K** 2003 NF-kappaB-mediated induction of p21(Cip1/Waf1) by tumor necrosis factor alpha induces growth arrest and cytoprotection in normal human keratinocytes. Mol Cancer Res 1:262-70
32. **Schroeder MD, Symowicz J, Schuler LA** 2002 PRL modulates cell cycle regulators in mammary tumor epithelial cells. Mol Endocrinol 16:45-57
33. **Zhao J, Pestell R, Guan JL** 2001 Transcriptional activation of cyclin D1 promoter by FAK contributes to cell cycle progression. Mol Biol Cell 12:4066-77

Fig.1

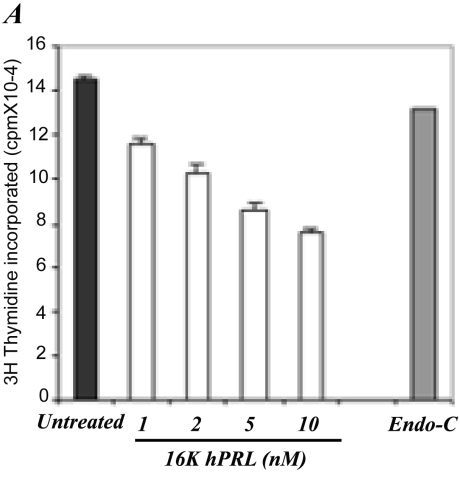

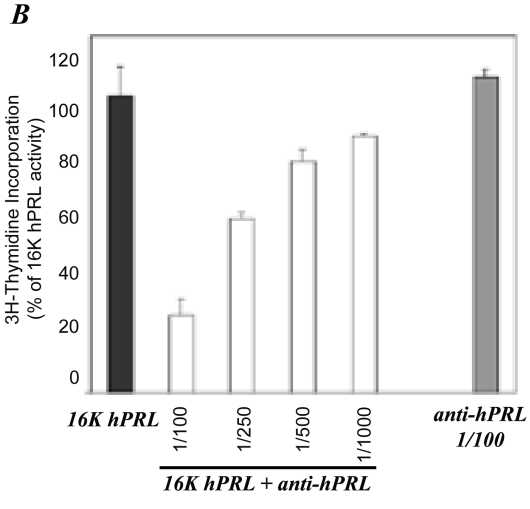

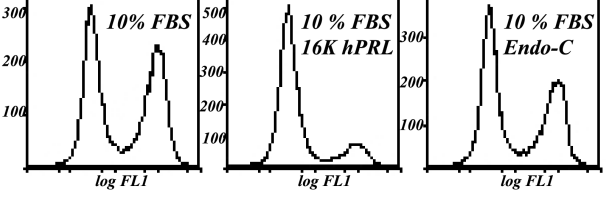

Treatment	Percentage of BrdU positive cell
O% FBS	29%
% FBS	49%
10% FBS + 16K hPRL	16%
10% FBS + Endo-C	42%

Fig.2

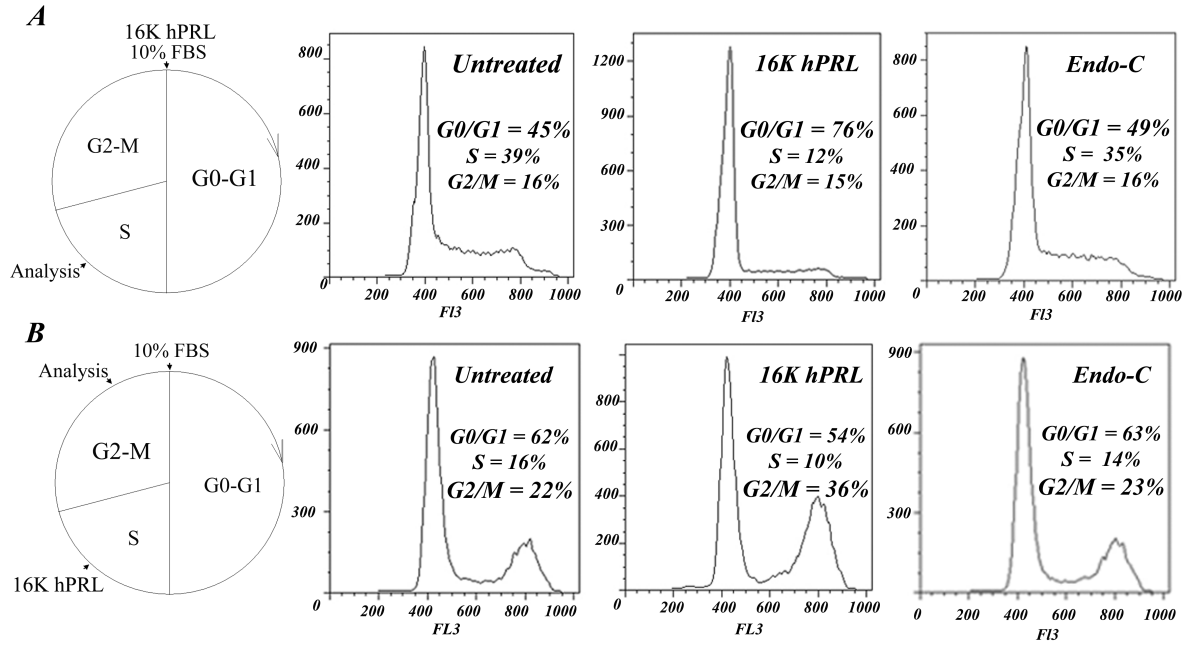
A
16K hPRL
10% FBS
G2-M
G0-G1
S
Analysis
Untreated
G0/G1 = 45%
S = 39%
G2/M = 16%
16K hPRL
G0/G1 = 76%
S = 12%
G2/M = 15%
Endo-C
G0/G1 = 49%
S = 35%
G2/M = 16%
Fl3
B
10% FBS
Analysis
G2-M
G0-G1
S
16K hPRL
Untreated
G0/G1 = 62%
S = 16%
G2/M = 22%
16K hPRL
G0/G1 = 54%
S = 10%
G2/M = 36%
Endo-C
G0/G1 = 63%
S = 14%
G2/M = 23%
FL3
Fl3

Fig 3

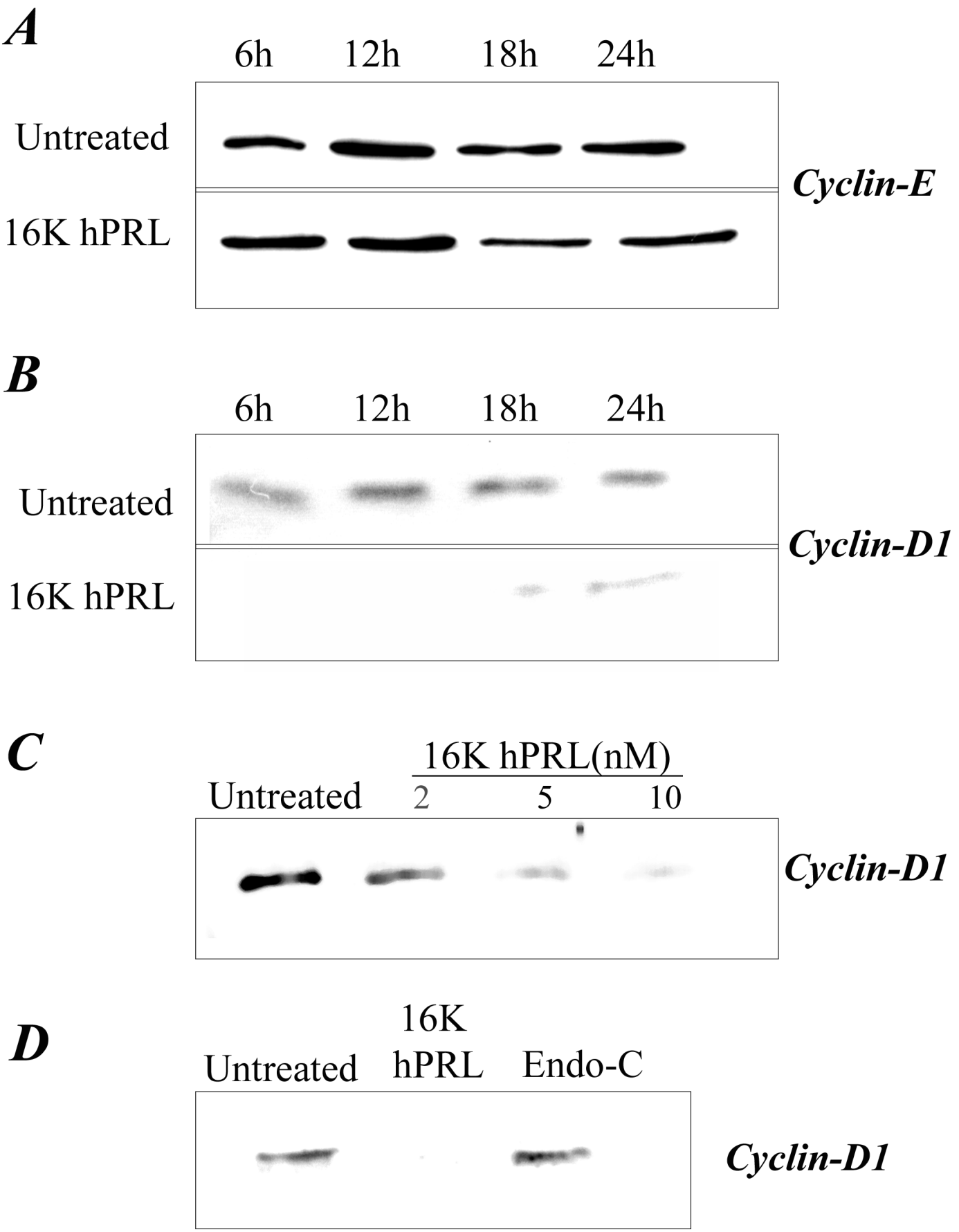
A
6h
12h
18h
24h
Untreated
16K hPRL
Cyclin-E
B
6h
12h
18h
24h
Untreated
16K hPRL
Cyclin-D1
C
16K hPRL(nM)
Untreated
2
5
10
Cyclin-D1
D
16K
Untreated
hPRL
Endo-C
Cyclin-D1

Fig 4

A

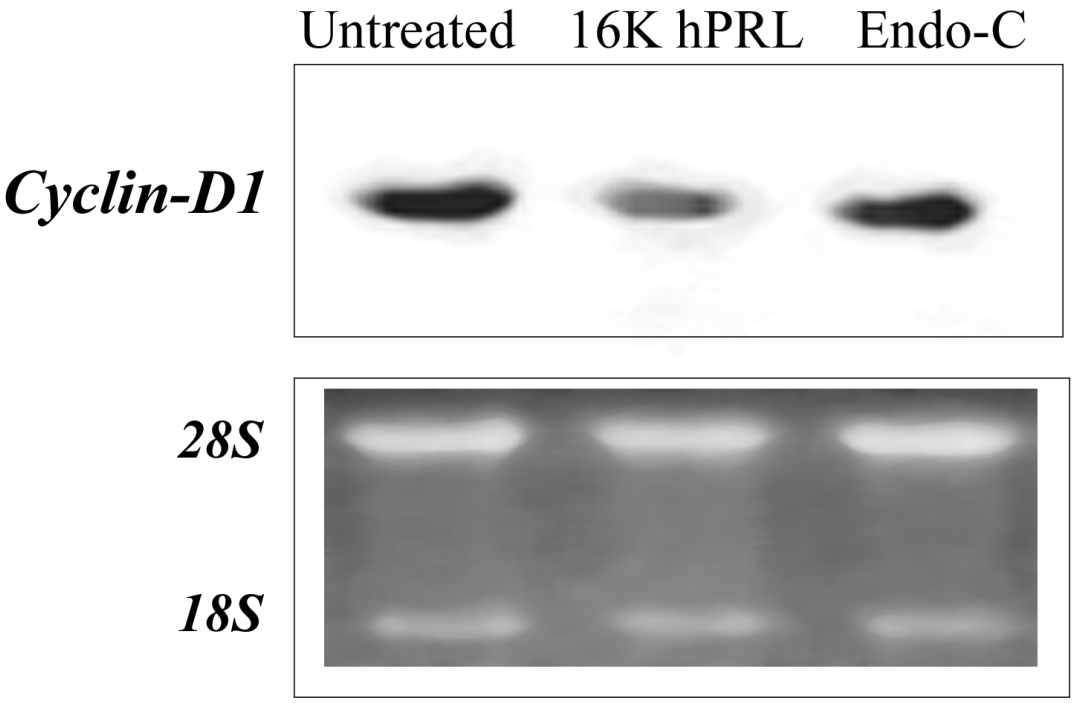
Untreated
16K hPRL
Endo-C
Cyclin-D1
28S
18S

B

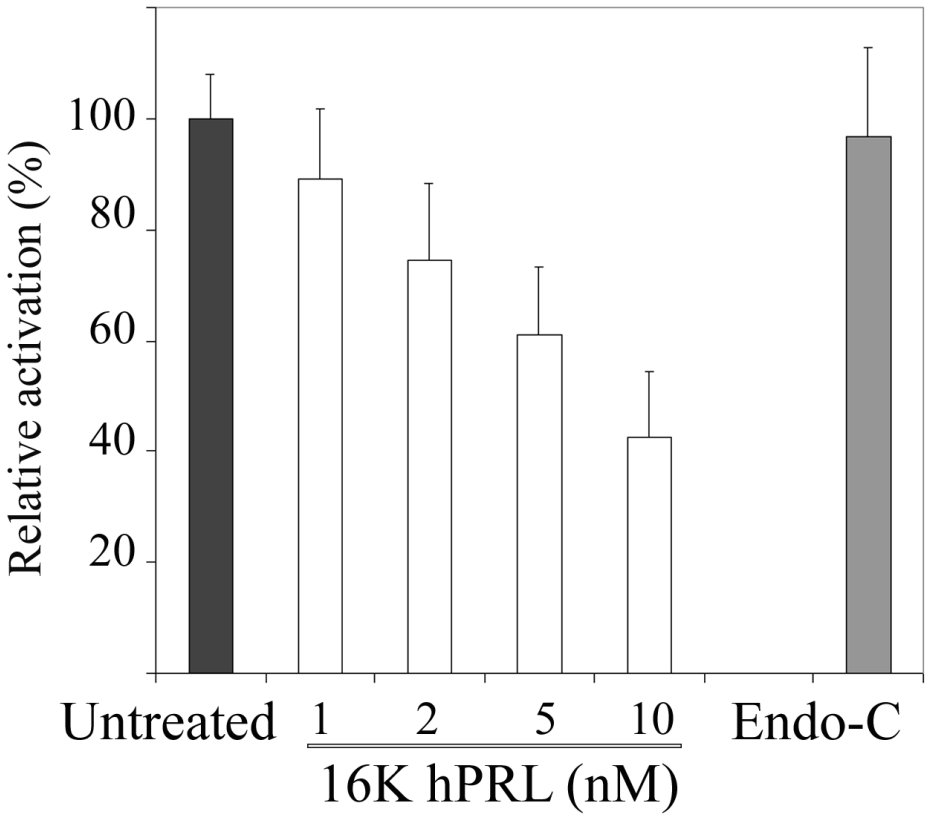
Relative activation (%)
100
80
60
40
20
Untreated
1
2
5
10
Endo-C
16K hPRL (nM)

Fig 5

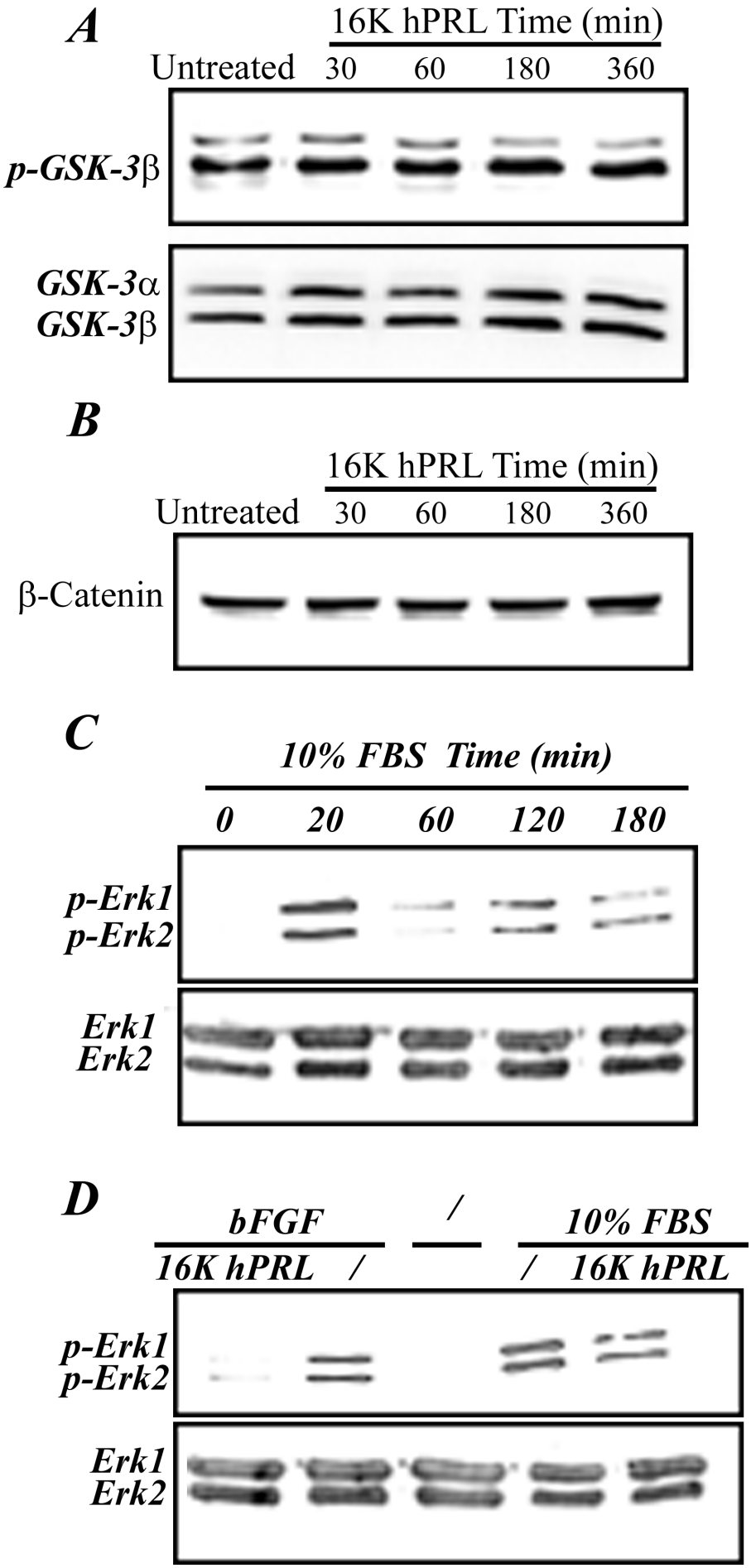
A
16K hPRL Time (min)
Untreated
30
60
180
360
p-GSK-3β
GSK-3α
GSK-3β
B
16K hPRL Time (min)
Untreated
30
60
180
360
β-Catenin
C
10% FBS Time (min)
0
20
60
120
180
p-Erk1
p-Erk2
Erk1
Erk2
D
bFGF
/
/
10% FBS
16K hPRL
/
/
16K hPRL
p-Erk1
p-Erk2
Erk1
Erk2

Fig 6

A

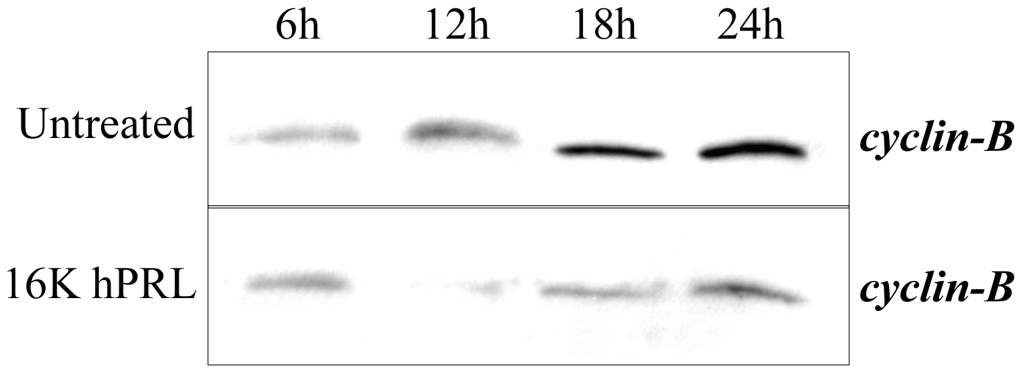
6h
12h
18h
24h
Untreated
cyclin-B
16K hPRL
cyclin-B

B

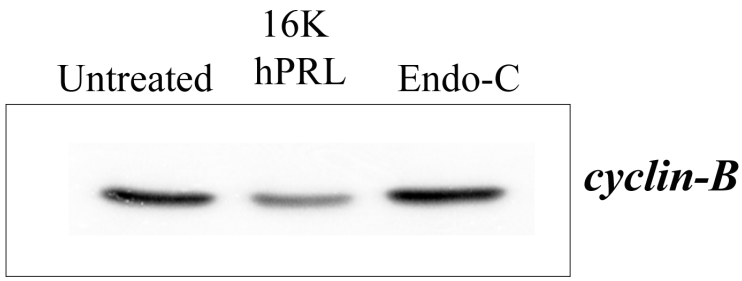
16K
hPRL
Untreated
Endo-C
cyclin-B

C

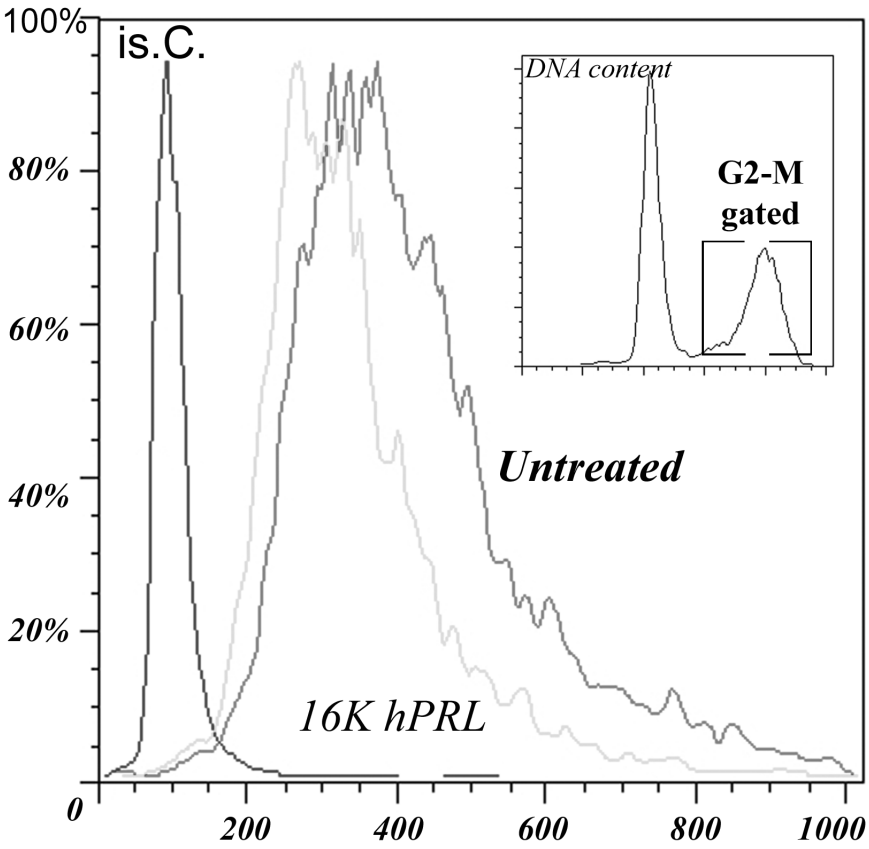
100%
80%
60%
40%
20%
0
is.C.
DNA content
G2-M
gated
Untreated
16K hPRL
200
400
600
800
1000

Fig 7

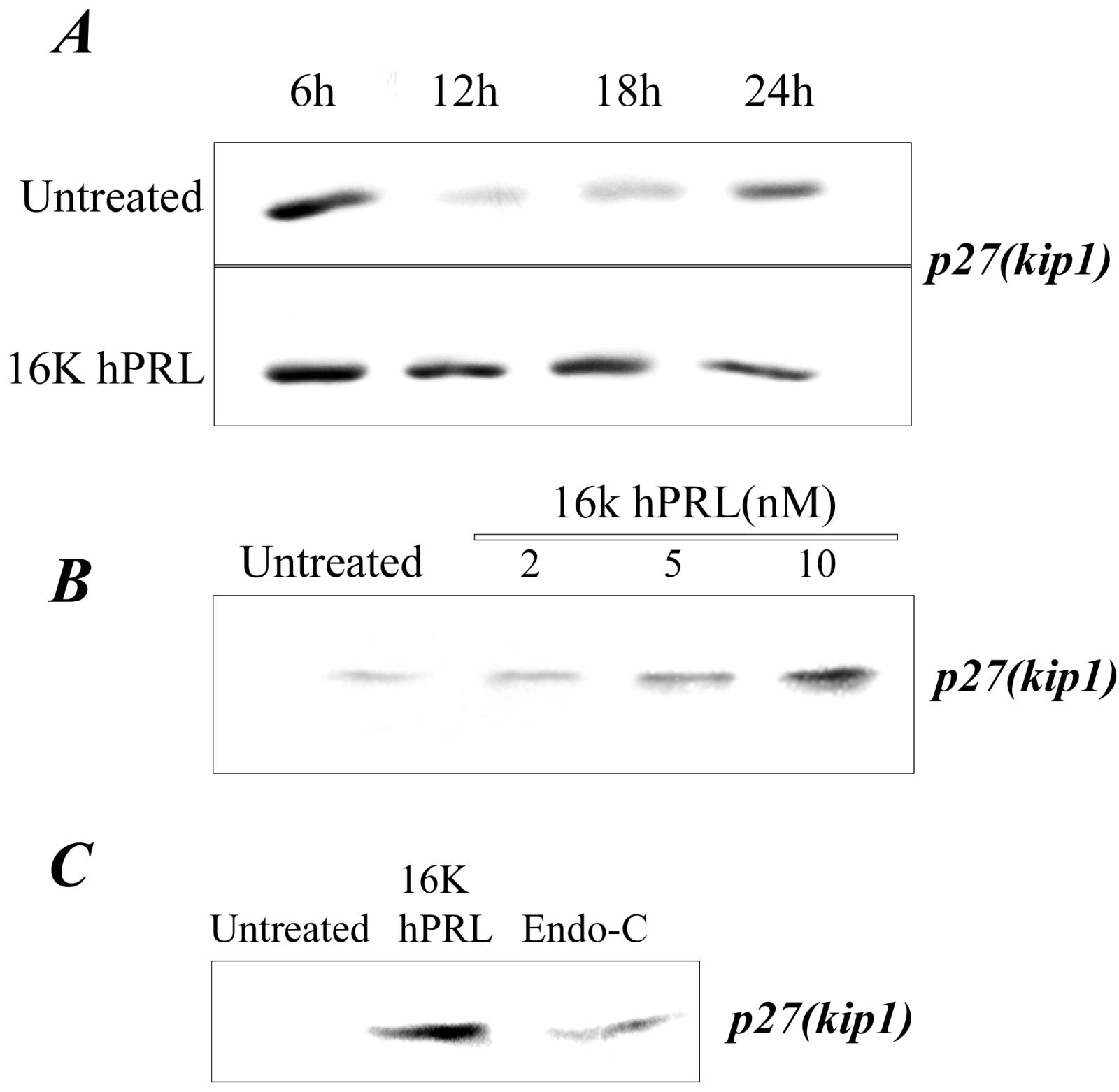
A
6h
12h
18h
24h
Untreated
16K hPRL
p27(kip1)
B
16k hPRL(nM)
Untreated
2
5
10
p27(kip1)
C
16K
Untreated
hPRL
Endo-C
p27(kip1)

Fig 8

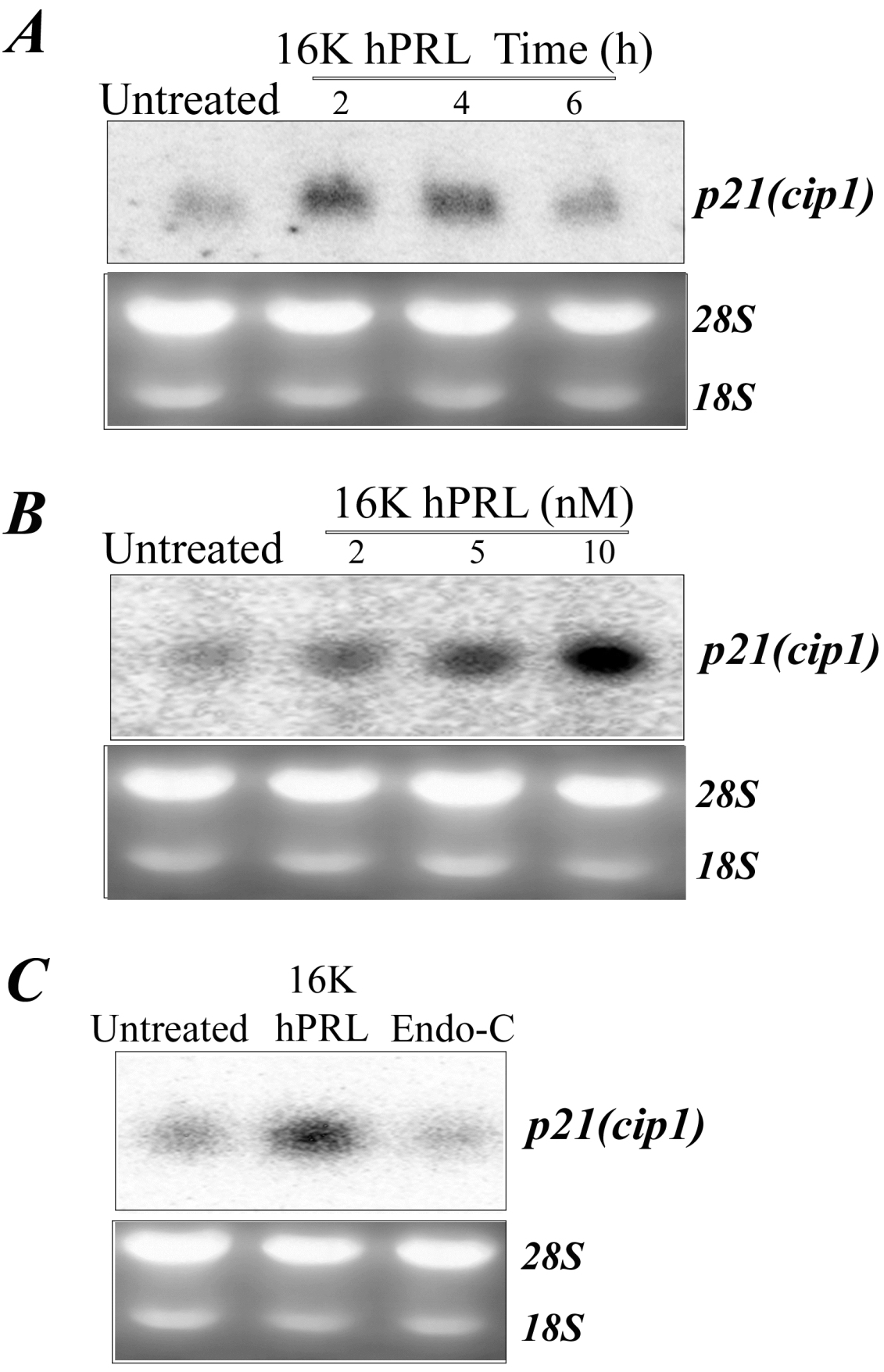
A
16K hPRL Time (h)
Untreated
2
4
6
p21(cip1)
28S
18S
B
16K hPRL (nM)
Untreated
2
5
10
p21(cip1)
28S
18S
C
16K
Untreated
hPRL
Endo-C
p21(cip1)
28S
18S